Journal of Materials Chemistry

Cite this: J. Mater. Chem., 2011, 21, 18199

www.rsc.org/materials

COMMUNICATION

Solar exfoliated graphene–carbon nanotube hybrid nano composites as efficient catalyst supports for proton exchange membrane fuel cells†

S. S. Jyothirmayee Aravind,[a] R. Imran Jafri,[a] N. Rajalakshmi[b] and S. Ramaprabhu*[a]

Received 11th August 2011, Accepted 10th October 2011
DOI: 10.1039/c1jm13908h

Ultra thin graphene–multi walled carbon nanotube composites prepared by a solar exfoliation technique have been explored as catalyst supports for oxygen reduction reaction (ORR) in proton exchange membrane fuel cells (PEMFC). Pt nanoparticles were dispersed on a solar exfoliated graphene-functionalized multi walled carbon nanotube (sG-fMWNT) hybrid nanocomposite, which exhibits higher electrocatalytic activity for ORR than Pt dispersed functionalized solar graphene (f-sG) catalyst support. The single cell PEMFC measurements give maximum power densities of 355 mW cm^{-2} and 675 mW cm^{-2} with sG and sG-f MWNT respectively. The improved performance in the power density with the sG-f MWNT fuel cell can be ascribed to the synergistic effect of 1D MWNT and 2D graphene in sG-f MWNT as well as its high electrochemical surface area. The inclusion of MWNT bridges the defects for electron transfer besides increasing the basal spacing between graphene sheets. The good performance and possibility of high throughput production of sG-f MWNT makes this material a promising catalyst support for PEMFC.

Introduction

Platinum nanoparticles have been considered the best catalysts for oxygen reduction reaction (ORR) in fuel cells for a long period. The limited reserves of Pt along with its high cost are hampering the commercialization of fuel cells even after its usage in the Apollo lunar mission in 1960.[1] Recent efforts in ORR electrocatalysis have focused on minimizing the Pt content by employing high surface area carbon nanomaterials.[2,3] A commodious support for an electrocatalyst should have a high surface area, good electrical properties and high electrochemical stability under PEM fuel cell operating conditions. Carbon supported electrocatalysts are found to be effective in maximizing the performance of proton exchange membrane fuel cells (PEMFC) and minimizing the use of noble metals such as Pt.[4–6] The efficacy of carbon support materials rely on the fact that they can maximize the availability of the nano sized electrocatalyst surface area and thus enhance the electron transfer. Conventionally, carbon black has been used as catalyst support for PEMFC due to its high surface area, high conductivity and low cost. In such systems, the catalytic performance loss during extended operations is a critical problem due to the degradation of catalyst particles and the corrosion of the cathode support.[7] Carbon nanotubes (CNT) potentially fulfil these requirements including a wide electrochemical potential window, good chemical stability and large surface area which make them attractive as electrode material candidates.[8]

The experimental realization of two dimensional graphene has opened a new channel for utilizing this 2D carbon material as a catalyst support in PEM fuel cells.[9,10] This two dimensional crystal of sp^2 hybridized carbon can be exfoliated from bulk graphite using micro mechanical cleavage,[11] thermal exfoliation,[12] and chemical reduction[13] techniques. Recently we showed that high conducting graphene can be synthesized by solar exfoliation of graphite oxide (GO).[14] The ability of graphene sheets to support nano particles open new ways to develop electrocatalysts for fuel cells. As-synthesized graphene, due to the removal of functional groups over the basal planes of GO, is highly hydrophobic and hence has to be functionalized to anchor Pt nanoparticles. But the process of functionalizing the graphene results in restacking of the graphene sheets, thus reducing the effective surface area. This can be avoided by using spacers and CNTs can be employed as space impediments between the graphene sheets to prevent the restacking of graphene. The combination of one-dimensional CNT and two-dimensional graphene can thus be exceptionally advantageous when employed as a catalyst support material in fuel cells. Taking this fact into consideration, we employ an *in situ* method of preparation of a hybrid composite material of graphene and multi walled carbon nanotubes (MWNT) by solar exfoliation of the GO–MWNT composite. We also report the deposition of Pt nanoparticles on solar exfoliated graphene (sG). The characterization of the Pt/sG as well as the Pt/sG–MWNT composite and evaluation of their electrocatalytic performance presented in this study provide an insight into the utilization of solar exfoliated graphene and novel hybrid solar graphene–MWNT composite as catalyst supports in PEMFC.

[a]*Alternative Energy and Nanotechnology Laboratory (AENL), Nanofunctional Materials Technology Centre (NFMTC), Department of Physics, Indian Institute of Technology Madras, Chennai, India. E-mail: ramp@iitm.ac.in; Fax: +91-44-22570509; Tel: +91-44-22574862*
[b]*Centre for Fuel Cell Technology, IIT Madras Research Park, Phase 1, II Floor, 6 Kanagam Road, Taramani, Chennai, 600 113, India*

† Electronic supplementary information (ESI) available: XRD of f-sG, f-MWNT and sG-f MWNT, FTIR of GO, sG, f-sG, f-MWNT, GO-f MWNT and sG-f MWNT, Inplane crystallite size from Raman spectra, Stability study of Pt/sG-f MWNT based fuel cell. See DOI: 10.1039/c1jm13908h

Experimental

GO was prepared from graphite by Hummer's method.[15] Graphene was prepared by the exfoliation of GO in the presence of focused solar radiation.[14] As prepared graphene was treated with conc. HNO_3 for 1h. This functionalized sG (f-sG) was used for Pt loading. MWNTs were prepared by a chemical vapour deposition method using acetylene as a carbon precursor.[16] As-grown MWNT were purified by heating in the air at 350 °C followed by refluxing in conc. HNO_3 for 24 h. Finally, the sample was washed with de-ionized water until it was pH neutral and dried at 60 °C. The purified MWNT was functionalized (f-MWNT) in a procedure similar to that of graphene. The solar graphene–MWNT composites was prepared by an *in situ* preparation technique which involves two steps. Initially, the f-MWNTs were refluxed with GO in conc. HNO_3 for 2h and washed in de-ionized water until they were pH neutral. The composite obtained is labelled GO-f MWNT. In the second step, the GO-f MWNT composite was solar exfoliated by harvesting and directing solar radiation towards it, using a convex lens with a diameter of 90 mm. The as-synthesized sG-f MWNT composite was used for the deposition of Pt nanoparticles without further functionalization.

Pt nanoparticles were loaded over the catalyst support materials by an ethylene glycol (EG) reduction method.[17] Briefly, the samples were placed into a flask and an ethylene glycol–water solution (2 : 1 volume ratio) was added. The metal precursor was a 0.01 M aqueous solution, and depending on the desired nano particle loading, an appropriate amount of the precursor was added. The flask was then placed on a hot plate with magnetic stirring. The reduction reactions were performed under reflux conditions (at 125 °C) for 2 h. The carbon nano materials with Pt nanoparticles on them were then separated from the ethylene glycol solution in the centrifuge and washed with de-ionized water several times. The Pt loading was kept constant *viz*. ~30 wt% for all samples. Fig. 1 demonstrates the synthesis of sG-f MWNT hybrid nanocomposite by solar exfoliation and subsequent deposition of Pt nanoparticles by EG reduction method. The samples were characterized using X-ray diffractogram (PANalytical X'Pert Pro X-ray diffractometer with a Cu-Kα radiation of 1.541 A°), Raman spectroscopy (Witec Raman microscope using green (532 nm) laser excitation, with excitation energy of 2.33 eV) and transmission electron microscopy (FEI Tecnai G^2 transmission electron microscope operated at 200 keV). Thermo gravimetric spectra were recorded with NETZSCH analyzer in air atmosphere with temperature heating of 10 °C min^{-1} and FTIR was performed on Perkin Elmer spectrum one spectrometer using KBr pellet method.

The membrane electrode assembly (MEA) was prepared by sandwiching a pretreated Nafion® 212 CS membrane between the anode and cathode, which comprised of a backing layer, a gas diffusion layer and a catalyst layer. The required amount of catalyst was coated over the electrodes after mixing them with the desired amount of Nafion and de-ionized water by ultrasonication. Briefly, 12 mg of Pt/f-MWNT (anode catalyst, 0.25 mg cm^{-2} loading) was mixed with 0.3 ml of 5 wt% Nafion and 25 mg of Pt/sG-f MWNT (cathode catalyst, 0.5 mg cm^{-2} loading) with 0.6 ml of 5 wt% Nafion. The suspension was coated homogeneously over the gas diffusion layer. The gas diffusion layer was formed by coating a mixture of Vulcan XC 72 carbon and poly tetra fluoro ethylene. The electrodes were sandwiched with Nafion membrane by hot pressing at 130 °C for 4 min. The second MEA was prepared in a similar route, by coating Pt/f-sG (0.5 mg cm^{-2} loading) over the cathode keeping Pt/f-MWNT (0.25 mg cm^{-2} loading) as the anode catalyst. The effective electrode area was 11.56 cm^2. The MEAs were tested in a fuel cell test station (ElectroChem Fuel Cell Test Station) by fixing them between two graphite plates which had a provision for gas flow (serpentine type). The H_2 gas at anode and O_2 gas at cathode were humidified by passing it through respective humidifiers and were controlled by their respective mass flow controllers (with flow rates of 100 sccm each).

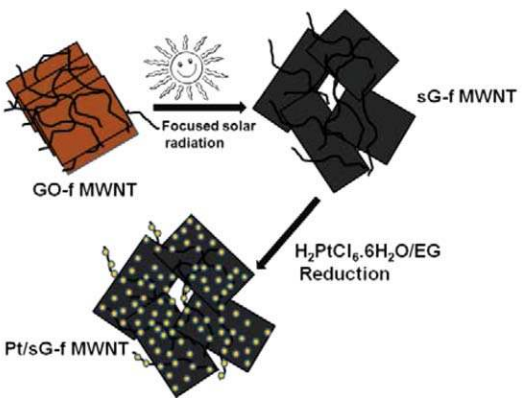

Fig. 1 Schematic for the preparation of Pt/sG-f MWNT.

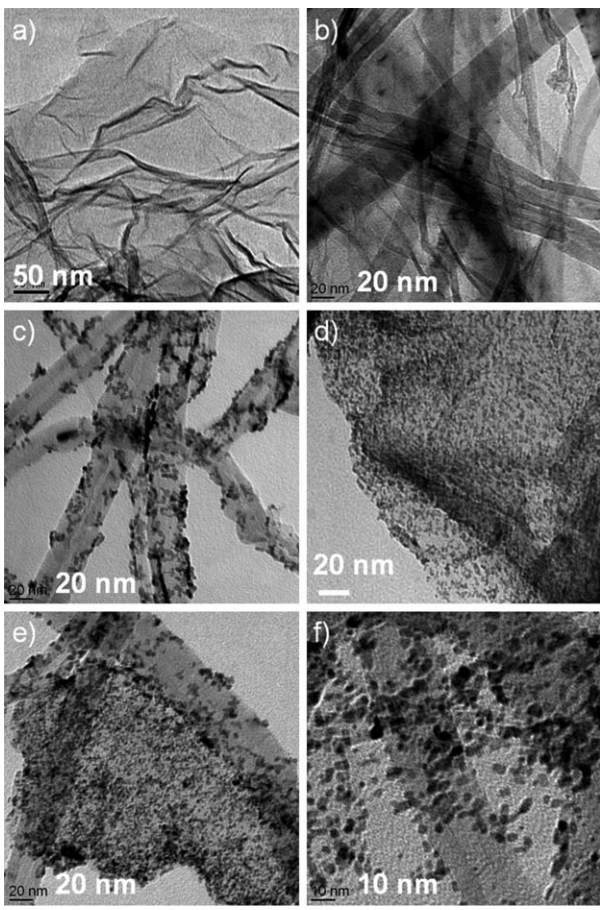

Fig. 2 HRTEM images of (a) f-sG (b) sG-f MWNT (c) Pt/f-MWNT (d) Pt/f-sG (e) low and (f) high magnification images of Pt/sG-f MWNT composite.

The morphological structure, particle size and the dispersion of Pt over the f-sG and sG-f MWNT have been analyzed by high resolution TEM. Fig. 2a displays f-sG as wrinkled sheets. Exfoliation of GO-f MWNT resulted in a mixture containing ultrathin graphene sheets embedded with f-MWNT (Fig. 2b). A typical TEM image of Pt dispersed functionalized MWNT (Pt/f-MWNT) in Fig. 2c shows that Pt nanoparticles of an average diameter of ~3.5 nm are uniformly decorated on the nanotubes. The Pt particle size on graphene is ~2.5 nm and the distribution is homogeneous over the graphene (Fig. 2d). The TEM image of Pt dispersed sG-fMWNT in Fig. 1e displays the uniform and full area distribution of Pt nano particles over graphene and f-MWNT. Further, the transparent nature of graphene in the sG-f MWNT composite prevents restacking of graphene in the presence of MWNT. The average particle diameter calculated from the high resolution TEM image (Fig. 2f) is ~3 nm.

The crystalline nature and average particle size were analyzed by X-ray diffraction. The XRD of f-sG shows a weak and broad peak C (002) around 25°, confirming the formation of graphene. A sharper and narrower carbon C (002) diffraction peak appear for MWNT, which indicates a highly graphitic ordered structure of MWNT. The spectrum of the sG-f MWNT composite exhibits a sharp peak at 26°, similar to that of f-MWNT (See ESI†). The XRD patterns of the Pt nanostructures (Fig. 3) are in good agreement with those of the reference patterns for face centered-cubic Pt (JCPDS 04-0802).[18] It is observed that the Pt on the three samples exhibits similar crystalline structures. The peaks at 39.7, 46.4, 67.7, and 81.1 can be indexed to Pt (111), (200), (220), and (311) diffraction peaks, respectively, confirming that the Pt nanostructures have a highly crystalline fcc phase. In addition, the average particle size of Pt nanoparticles calculated using the Scherrer equation are 3.5 nm, 2.5 nm and 3.1 nm for Pt/f-MWNT, Pt/f-sG and Pt/sG-f MWNT respectively, which is consistent with the TEM results.

The raman spectra of graphene and MWNT (Fig. 4) are characterized by two prominent features, a G band at ~1567 cm^{-1} arising due to first order Raman scattering of the E_{2g} phonon at the Brillouin zone center of the sp^2 carbon atoms[11,19] and a D mode at 1356 cm^{-1} arising from the breathing mode of κ-point phonons of A_{1g} symmetry, which requires a defect for its activation.[20] The ratio of the intensity of the G-band to the D-band is related to the in-plane crystallite size, La.[21] The in-plane crystallite size from the spectra corresponding to different samples has been calculated by employing the ratio, $La = 4.4/(I_D/I_G)$. Table S1, ESI,† compares the in plane crystallite size of f-sG and sG-f MWNT. The smaller La value of the sG-f MWNT composite is advantageous for its electrochemical applications.

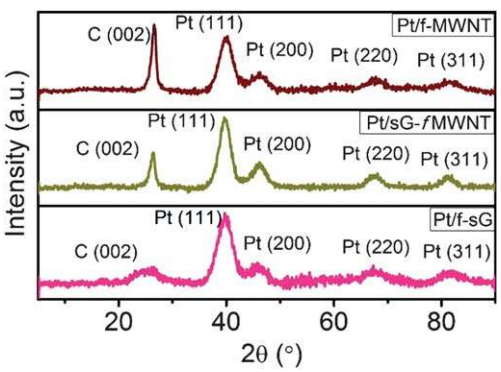

Fig. 3 XRD spectra of Pt/f-MWNT, Pt/sG-f MWNT and Pt/f-sG.

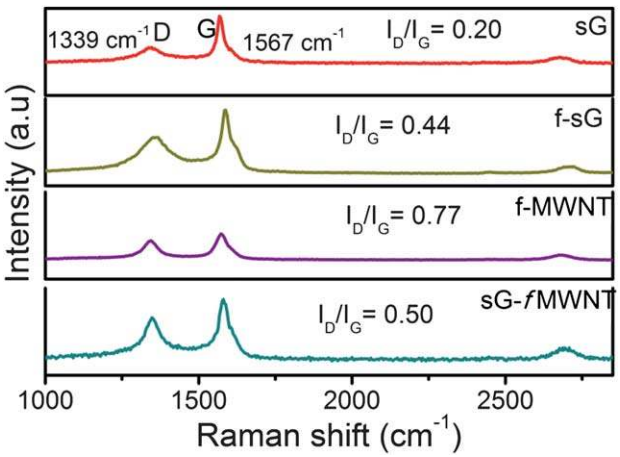

Fig. 4 Raman spectra of sG, f-sG, f-MWNT and sG-f MWNT.

After the Pt loading using EG reduction method, the TGA spectra of Pt/f-MWNT, Pt/f-sG and Pt/sG-f MWNT in air atmosphere were performed (Fig. 5) in order to analyze the loading level of Pt nanoparticles. As can be seen, the mass loadings of Pt on the different substrates were determined as 31.3 wt%, 31.7 wt% and 29.02 wt% for Pt/f-MWNT, Pt/sG-f MWNT and Pt/f-sG respectively. TGA spectra corroborate the experimental procedure of constant loading of Pt over different carbon supports.

The electrochemically active surface area (ECSA) was measured by scanning the electrocatalyst deposited electrode between −0.2 and 1.2 V (*vs* Ag/AgCl) in 1M H_2SO_4 solution at a scan rate of 10 mV s^{-1} (Fig. 6). The experiment was performed until a stable hydrogen desorption peak was observed. The cyclic voltammograms (CVs) of the catalysts clearly show hydrogen adsorption/desorption on Pt between ~ −0.17 and ~0.04 V followed by a double layer region and Pt–OH formation and reduction in the voltage range from 0.6–0.85 V *vs.* Ag/AgCl, which is in good agreement with the previous studies.[22] The catalyst surface available for charge transfer as well as the conductive path to transfer the electrons to and from the electrode surface can be estimated from ECSA. The integrated area under the desorption peak in CV can be used to calculate the total charge relating to H^+ desorption, Q_H and can be used to determine ECSA by the relation:[23]

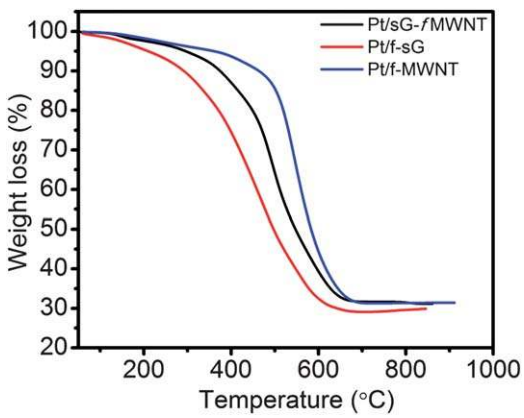

Fig. 5 TGA analysis curves of Pt/f-sG, Pt/f-MWNT and Pt/sG-f MWNT.

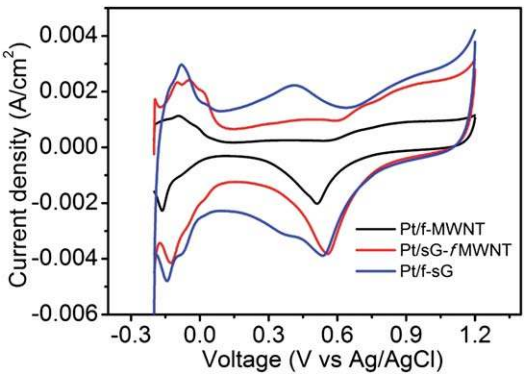

Fig. 6 Cyclic voltammograms of the electrocatalysts recorded at a scan rate of 10 mV s^{-1}. The current normalization has been done with geometric area of the electrode (0.07 cm^2).

$$\mathrm{ECSA} = Q_H/0.21 \text{ x } [\mathrm{Pt}]$$

where, [Pt] represents the loading of Pt (0.21 mg cm^{-2}) and 0.21(mC cm^{-2}) is the charge required to oxidize a monolayer of H_2 on the Pt site.[24] It is interesting to note that the CV of Pt dispersed hybrid nanocomposite is different from that of the pure catalyst supports. This can be due to the various crystalline (hkl) planes or differences in the shape of the nanoparticles.[25] Considering different hydrogen desorption energies for different planes, each peak in the CV pattern accords to a particular plane of Pt nanoparticle. In the CV of hybrid nanocomposite based electrocatalyst, the prominent peaks correspond to the Pt–H adsorption/desorption on Pt (111) and Pt (110) facets respectively, whereas in the case of electocatalysts with pure supports, the peak corresponding to Pt (111) is absent and peak corresponding to Pt (110) plane is pronounced. Hence, it is asserted that the use of hybrid nanocomposites as catalyst support governs the morphology of Pt nanoparticles produced. Table 1 summarizes the ECSA values of different electrocatalysts. The ECSA of sG-f MWNT supported Pt is higher than both sG and MWNT supported Pt. These results indicate that Pt/sG-f MWNT is a good catalyst for PEMFC with higher ECSA of Pt than Pt/f-sG or Pt/f-MWNT, which can be attributed to the uniform dispersion of Pt particles on the hybrid nanostructure and good accessibility of these sites for hydrogen adsorption and desorption reactions. Hence, it can be concluded that Pt dispersed sG-f MWNT nano composites can be a good candidate for the oxygen reduction reaction (ORR) in PEMFC.

Table 1 summarizes the ECSA and Pt utilization of different cathode catalysts used, where d is the average particle size (nm) and ρ the Pt density (21.4g cm^{-3}).[25] Platinum utilization (%) is defined and calculated as the ratio of ECSA and specific surface area of Pt. The ECSA values of Pt nanoparticles in sG-f MWNT hybrid nanomaterial is in very good agreement with the apparent specific surface area estimated from XRD data, suggesting that approximately 82% of the apparent specific surface area is electrochemically active. It is observed that the percentage utilization is maximum for the Pt dispersed hybrid nanocomposite based electrocatalyst. The graphene sheets tend to agglomerate at the electrode surface upon solvent evaporation. This feature paves the way for the restacking of the graphene sheets due to van der Waals attraction and therefore decreasing the surface area accessible for the redox probe.[26] This may considerably decrease the electrocatalytic activity of the Pt/f-sG. On the other hand, MWNTs in the hybrid nanocomposite act as a space impediment between the graphene layers, thereby ensuring their efficient separation.[25] Pt nanoparticles are dispersed over these well separated MWNTs and the graphene, ensuring large surface area of the hybrid nano composite and hence high Pt utilization.

Fig. 7 shows the polarization curves at three different temperatures for membrane electrode assembly (MEA) prepared with Pt/f-sG as the cathode catalyst with a loading of 0.5 mg cm^{-2}. Pt/f-MWNTs with 0.25 mg cm^{-2} loading was employed as the anode catalyst in all the MEAs in the present study. The performance of this MEA was tested using the fuel cell test station. Prior to the polarization studies, the electrodes were activated between open circuit potential and high current densities in order to activate the catalyst for the oxygen reduction reaction. The polarization plots were recorded using a dc load box. The f-sG based fuel cell exhibits an open circuit voltage of 0.94 V. A maximum power density of 260 mW cm^{-2} was obtained at 40 °C. It is observed that the cell performance greatly increases when the temperature increases because the catalyst activity and the diffusion coefficient of the reactant and the resultant increase with increasing temperature. At 50 °C, the power density is 304 mW cm^{-2} and a maximum power density of 355 mW cm^{-2} is attained at 60 °C with Pt/f-sG based MEA. This is higher than the reported values of

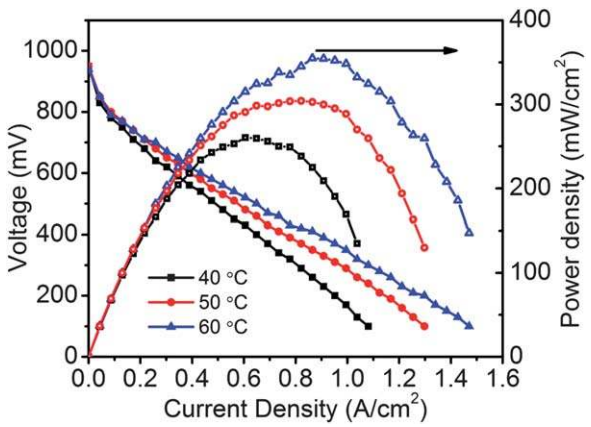

Fig. 7 Polarization graph of Pt/f-sG (cathode catalyst) and Pt/f-MWNT (anode catalyst).

Table 1 Comparison of electrocatalytically active surface area (ECSA) of different electrocatalysts

Electrocatalyst	Particle size from XRD, d (nm)	Specific surface area (m^2 g^{-1})	ECSA (m^2 g^{-1})	Pt utilization (%)
Pt/f-MWNT	3.2 ± 0.2	87 ± 14	61	70
Pt/f-sG	2.1 ± 0.2	133 ± 14	65	49
Pt/sG-fMWNT	2.8 ± 0.3	100 ± 9	82	82

161 mW cm^{-2} for partially reduced GO-Pt[27] and 195 mW cm^{-2} for Pt/G prepared by chemical method.[3]

The polarization data and power densities obtained with the Pt/sG-f MWNT catalyst based MEA at 40 °C, 50 °C and 60 °C is shown in Fig. 8. The uniform dispersion of the electrocatalyst on a graphene–MWNT mixture has been found to be congruous for achieving relatively better performance in fuel cells. The maximum power densities with this cell were 592, 657 and 675 mW cm^{-2} at 40, 50 and 60 °C respectively. The better performance with the Pt/sG-f MWNT electrocatalysts compared to the Pt/f-sG electrocatalysts is in conformity with the larger ECSA of Pt in Pt/sG-f MWNT, demonstrating a better electrocatalytic activity of the Pt/sG-f MWNT compared to Pt/f-sG and Pt/f-MWNT. The enhancement in power density with the hybrid nano composite based MEA can be attributed to the synergistic effect of 1D MWNT and 2D graphene. The van der Waals force between graphitic layers actuates them to restack to form a graphitic structure. The addition of MWNT not only bridges the defects for electron transfer but also increases the basal spacing between graphene sheets possibly due to the electronic affinity of MWNT.[28] Also, it is reported that the hybrid nanocomposite may increase the available triple phase boundary, which is a crucial factor for PEMFC.[29] The performance of the solar exfoliated graphene–MWNT based MEA is higher than the reported value of 540 mW cm^{-2} using a graphene–MWNT composite prepared by chemical methods.[25] The current technique possesses many advantages such as the one step preparation technique of the catalyst support and hence, agglomeration of graphene sheets can be efficiently prevented in the presence of MWNT. This is evident from the HRTEM image of Pt/sG-f MWNT, where the uniform deposition of Pt nanoparticles over an ultrathin graphene sheet embedded MWNT structure is clearly visible. Moreover, the EG reduction technique employed for the deposition of Pt nanoparticles results in a more uniform deposition of Pt nanoparticles over the catalyst support. This in turn, enhances the electrocatalyst–carbon support interaction which leads to the efficient utilization of the catalyst particles in the anode and cathode for the fuel cell reaction.

The difference in cell performances with different cathode catalysts is now considered. In PEMFCs, when increasing the current density, a decrease of cell potential is observed due to activation, ohmic, and concentration polarizations. If the decrease is minimal, fuel cell performance is good and the maximum power density of the cell is achieved. In the present work, better performance in the activation-controlled region (low current density) of Pt/sG-fMWNT compared to that of Pt/f-sG may be attributed to the enhanced specific activity of Pt due to the unique interaction of Pt and the sG-fMWNT support.[30] The possibly improved electron transfer through both sG and MWNT in the sG-fMWNT catalyst layer may help to enhance Pt utilization and reduce ohmic resistance of the electrode, which can provide improved performance over the entire current density range. At the mass transfer controlled region (high current density), the presence of comparatively hydrophobic sG helps to repel water from the cathode in the case of the Pt/sG-f MWNT fuel cell, whereas the MEA with f-sG shows lower performance that may be due to 'flooding' of the electrode, resulting in mass transport difficulty. Hence, it may be concluded that when Pt/sG-f MWNT is used as the cathode, higher PEMFC performance is achieved because of improved Pt utilization and mass transport. The histogram in Fig. 9 provides a comparison of the performance of electrocatalysts in this study with a state of the art commercial Pt/C catalyst,[31] partially reduced GO-Pt,[27] Pt/G produced by chemical method,[3] Pt/MWNT[25] and Pt dispersed over graphene–MWNT (Pt/f-G-f-MWNT) by a chemical method.[25]

To further substantiate the effect of oxygen adsorption, a back-pressure of 1 atm at the cathode of Pt/sG-f MWNT based fuel cell has been applied (Fig. 10). With the application of oxygen backpressure, the Pt/sG-f MWNT based fuel cell exhibits better performance. The

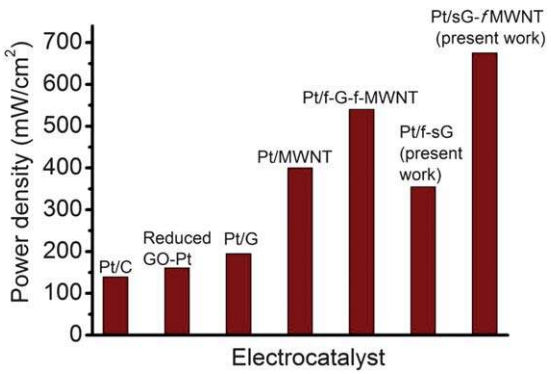

Fig. 9 Comparison of power density obtained with various ORR electrocatalysts.

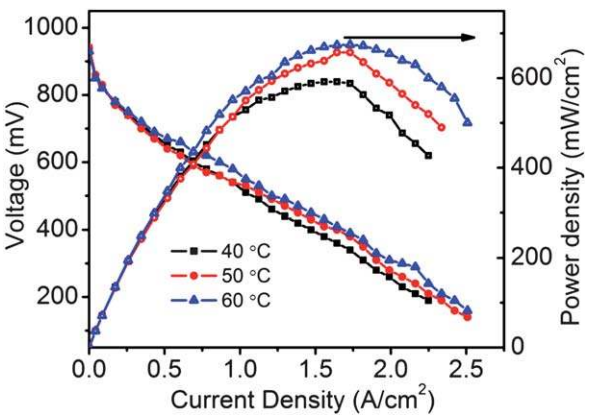

Fig. 8 Polarization graph of Pt/sG-f MWNT (cathode catalyst) and Pt/f-MWNT (anode catalyst) without back pressure.

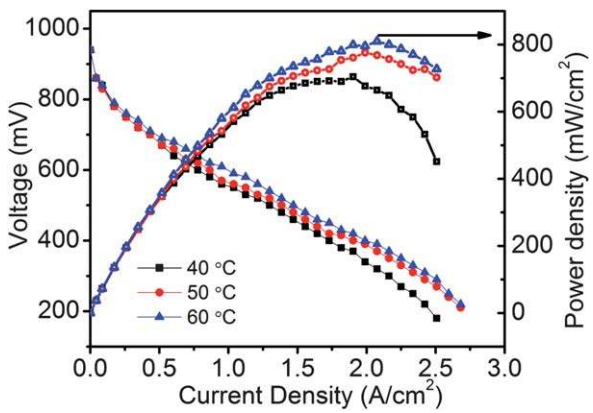

Fig. 10 Polarization graph of Pt/sG-f MWNT (cathode catalyst) and Pt/f-MWNT (anode catalyst) with 1 atm back pressure.

possible reasons include a stronger adsorption and hence interaction with the catalyst support and reduced activation energies for oxygen adsorption/oxidation and improved mass transfer with Pt dispersed sG-f MWNT electrocatalyst. The maximum power densities at 40, 50 and 60 °C were 704, 742 and 781 mW cm^{-2} respectively.

Conclusions

In summary, the practical application of graphene and a graphene–MWNT composite, prepared by simple solar exfoliation have been demonstrated. The maximum power density of Pt/f-sG catalyst (260 mW cm^{-2} at 540 mV) is higher than that of the state of the art commercial Pt/C catalyst (139 mW cm^{-2} at 540 mV). Moreover, the maximum power density of the Pt/sG-f MWNT is 675 mW cm^{-2}, which is 1.9 times higher than Pt/f-sG (355 mW cm^{-2}). The enhanced performance of the sG-f MWNT composite as a catalyst support compared to pure f-sG has been ascribed to the bridging of defects for the electron transfer and an increase in the basal spacing between graphene sheets with the incorporation of MWNT. The present low cost solar graphene and solar graphene–MWNT hybrid composite hold great promise for applications in energy devices such as fuel cells and batteries.

Acknowledgements

The authors S. S. Jyothirmayee Aravind, R. Imran Jafri, and S. Ramaprabhu thank IITM for the support.

Notes and references

1 Fuel Cells. http://americanhistory.si.edu/fuelcells/alk/alk3.htm.
2 Y. Hu, H. Zhang, P. Wu, H. Zhang, B. Zhou and C. Cai, *Phys. Chem. Chem. Phys.*, 2011, **13**, 4083–4094.
3 Y. Si and E. T. Samulski, *Chem. Mater.*, 2008, **20**, 6792–6797.
4 H. Chang, S. H. Joo and C. Pak, *J. Mater. Chem.*, 2007, **17**, 3078–3088.
5 W. Zhang, P. Sherrell, A. I. Minett, J. M. Razal and J. Chen, *Energy Environ. Sci.*, 2010, **3**, 1286–1293.
6 B. Seger and P. V. Kamat, *J. Phys. Chem. C*, 2009, **113**, 7990–7995.
7 Y. Shao, J. Liu, Y. Wang and Y. Lin, *J. Mater. Chem.*, 2009, **19**, 46–59.
8 A. L. Dicks, *J. Power Sources*, 2006, **156**, 128–141.
9 Y. Hu, H. Zhang, P. Wu, H. Zhang, B. Zhou and C. Cai, *Phys. Chem. Chem. Phys.*, 2011, **13**, 4083–4094.
10 E. Yoo, T. Okada, T. Akita, M. Kohyama, I. Honma and J. Nakamura, *J. Power Sources*, 2011, **196**, 110–115.
11 K. S. Novoselov, A. K. Geim, S. V. Morozov, D. Jiang, Y. Zhang, S. V. Dubonos, I. V. Grigorieva and A. A. Firsov, *Science*, 2004, **306**, 666–669.
12 H. C. Schniepp, J.-L. Li, M. J. McAllister, H. Sai, M. Herrera-Alonso, D. H. Adamson, R. K. Prud'homme, R. Car, D. A. Saville and I. A. Aksay, *J. Phys. Chem. B*, 2006, **110**, 8535–8539.
13 S. Park and R. S. Ruoff, *Nat. Nanotechnol.*, 2009, **4**, 217–224.
14 V. Eswaraiah, S. S. Jyothirmayee Aravind and S. Ramaprabhu, *J. Mater. Chem.*, 2011, **21**, 6800–6803.
15 W. S. Hummers and R. E. Offeman, *J. Am. Chem. Soc.*, 1958, **80**, 1339–1339.
16 A. L. M. Reddy, M. M. Shaijumon and S. Ramaprabhu, *Nanotechnology*, 2006, **17**, 5299–5305.
17 Y. Xing, *J. Phys. Chem. B*, 2004, **108**, 19255–19259.
18 J. Xu, T. Zhao, Z. Liang and L. Zhu, *Chem. Mater.*, 2008, **20**, 1688–1690.
19 M. S. Dresselhaus, A. Jorio, M. Hofmann, G. Dresselhaus and R. Saito, *Nano Lett.*, 2010, **10**, 751–758.
20 A. C. Ferrari and J. Robertson, *Phys. Rev. B: Condens. Matter*, 2000, **61**, 14095–14107.
21 K. S. Subrahmanyam, S. R. C. Vivekchand, A. Govindaraj and C. N. R. Rao, *J. Mater. Chem.*, 2008, **18**, 1517–1523.
22 J. Zhang, K. Sasaki, E. Sutter and R. R. Adzic, *Science*, 2007, **315**, 220–222.
23 M. Sogaard, M. Odgaard and E. M. Skou, *Solid State Ionics*, 2001, **145**, 31–35.
24 S. J. Lee, S. Mukerjee, J. McBreen, Y. W. Rho, Y. T. Kho and T. H. Lee, *Electrochim.Acta*, 1998, **43**, 3693–3701.
25 R. I. Jafri, T. Arockiados, N. Rajalakshmi and S. Ramaprabhu, *J. Electrochem. Soc.*, 2010, **157**, B874–B879.
26 H. Liu, J. Gao, M. Xue, N. Zhu, M. Zhang and T. Cao, *Langmuir*, 2009, **25**, 12006–12010.
27 B. Seger and P. V. Kamat, *J. Phys. Chem. C*, 2009, **113**, 7990–7995.
28 Z. Fan, J. Yan, L. Zhi, Q. Zhang, T. Wei, J. Feng, M. Zhang, W. Qian and F. Wei, *Adv.Mater.*, 2010, **22**, 3723–3728.
29 T. Matsumoto, T. Komatsu, K. Arai, T. Yamazaki, M. Kijima, H. Shimizu, Y. Takasawa and J. Nakamura, *Chem. Commun.*, 2004, 840–841.
30 C. A. Bessel, K. Laubernds, N. M. Rodriguez and R. T. K. Baker, *J. Phys. Chem. B*, 2001, **105**, 1115–1118.
31 A. L. M. Reddy and S. Ramaprabhu, *J. Phys. Chem. C*, 2007, **111**, 16138–16146.

